

Constraints on the Formation of Sedimentary Dolomite

Abstract. *The experimental replacement of calcite and aragonite by dolomite under a variety of conditions indicates that dolomitization can take place in marine and lacustrine environments under two conditions: (i) low dissolved sulfate concentrations and (ii) insubstantial contemporaneous silica diagenesis. Common sites for dolomite formation are areas where the dissolved sulfate concentration is reduced by microbial sulfate reduction, through the mixing of seawater with large amounts of fresh water, or where low-sulfate alkaline lacustrine environments prevail. Even under these conditions, dolomite formation may be inhibited by the concurrent transformation of opal-A (amorphous silica) to opal-CT (disordered cristobalite and tridymite), whereas the subsequent transformation of opal-CT to quartz favors the formation of dolomite.*

The problems of the origin of dolomite, $\text{CaMg}(\text{CO}_3)_2$, and the chemical conditions promoting the dolomitization of limestones have been debated at length. Dolomite is the thermodynamically stable carbonate phase in seawater, but it is a rather rare mineral in recent deep-sea calcareous sediments. By contrast, dolomite is an abundant constituent of ancient carbonate rocks now exposed on land.

Interest in the problem was revived recently when extensive dolomite formation was found to occur in continental margin sediments (1). Dolomitized limestones are also important oil reservoir rocks. A survey of dolomite occurrences in cores of the Deep Sea Drilling Project (DSDP) (2) revealed the following main features: (i) Dolomite rhombs occur commonly in pelagic sediments but only rarely in substantial quantity. In most cases, it is not known if these rhombs are detrital or diagenetic in origin. (ii) Dolomite is often associated with recrystallized biogenic silica (chert and porcelainite) or altered volcanic debris. (iii) Dolomite is an important component of organic-rich marine sediments, including very young sediments from the Gulf of California (3).

This report presents evidence from laboratory experiments on the chemical controls of the dolomitization reaction. These results permit a consistent explanation

for the formation of dolomite in certain oceanic environments, as well as in supratidal-evaporative (for example, sabkha), supratidal-nonevaporative, alkaline lacustrine, and groundwater settings, and for the absence of dolomite in apparently favorable environments, for example, open marine settings.

Several syntheses of dolomite were conducted at 200°C in Teflon-lined stainless steel bombs at equilibrium vapor pressure. Precipitated calcite (Baker reagent grade) with a BET (Brunauer, Emmett, and Teller) surface area of 0.51 m^2/g was used as a starting material. In some measurements Ludox silica with a BET surface area of 61 m^2/g was admixed. Ten milliliters of various starting solutions (Tables 1 through 4) were then pipetted into reaction vessels. The vessels were sealed and placed in an oven for the specified duration of the experiment. Then the samples were immediately filtered through 0.45- μm Millipore filters, and the solids and solutions were analyzed. Routine analyses included x-ray diffraction and scanning electron microscopy of the solid phases and Ca^{2+} , Mg^{2+} , alkalinity, Cl^- , and silica determinations of the solutions (4). Selected experimental conditions and results are given in Tables 1 through 4.

The experiments in Table 1 established the approximate boundaries of the dolomite stability field as a function of

the $\text{Mg}^{2+}/\text{Ca}^{2+}$ molar ratio at seawater ionic strength ($I = 0.7$) at 200°C. These experiments lasted 2 weeks, probably sufficient time for the establishment of phase equilibrium. The calcite-dolomite phase boundary occurs at a $\text{Mg}^{2+}/\text{Ca}^{2+}$ molar ratio between 0.57 and 1.06, and the dolomite-magnesite boundary between 2.11 and 3.41.

For the experiments in Table 2 we used as starting solution 0.080M MgCl_2 + 0.060M CaCl_2 + 0.280M NaCl to determine the time necessary for replacement of the initial CaCO_3 by dolomite at 200°C. With calcite as the starting material, replacement by ordered dolomite was complete between 4.7 and 6.7 days; with aragonite as the starting material (5), total replacement was achieved in less than 2 days. Dolomitization proceeded through a 46 mole percent magnesium protodolomite intermediate phase (6).

The experiments in Table 3 were conducted to determine the effect of dissolved SO_4^{2-} on dolomite formation from calcite. The addition of even minor amounts of dissolved SO_4^{2-} strongly inhibited the rate and degree of calcite dolomitization under the experimental conditions. In this series also ordered dolomite formed through a protodolomite precursor. Preliminary experimental results indicate that dolomitization of aragonite proceeds at somewhat higher dissolved SO_4^{2-} concentrations than that of calcite. The same effects have been observed in experiments conducted at 100°C.

The experiments in Table 4 demonstrated the effect of admixed Ludox silica powder on the dolomitization (or magnesitization) process. Neither dolomite nor magnesite formed; instead, Mg^{2+} reacted with silica to form opal-CT (7). Table 4 shows that the amorphous silica transformation to opal-CT depressed the Mg^{2+} content of the solutions to such a degree that the $\text{Mg}^{2+}/\text{Ca}^{2+}$ ratio necessary for dolomite formation (Table 1) was never reached.

Rosenberg and Holland (8) and Udowski (9) defined the magnesite-dolomite-calcite phase boundaries experimentally between 120° and 420°C in high ionic strength solutions. Rosenberg and Holland's (8) data indicate that at 200°C the molar $\text{Mg}^{2+}/\text{Ca}^{2+}$ ratio of the calcite-dolomite boundary is 0.14. In solutions of lower ionic strength (comparable to those in our study) the rate of dolomitization was slower, and the phase boundaries of magnesite-dolomite and dolomite-calcite were shifted to higher molar $\text{Mg}^{2+}/\text{Ca}^{2+}$ ratios (8, 10). Katz and Matthews (11) dolomitized calcite through an

Table 1. Dolomitization of calcite (20 mg reagent grade) in 10 ml of MgCl_2 + CaCl_2 + NaCl solution ($I = 0.7$) at 200°C; M, magnesite; P, protodolomite; D, dolomite; C, calcite. The duration of the experiment was 2 weeks. The mole percentage of magnesium was determined by x-ray diffraction (6).

$\text{Mg}^{2+}/\text{Ca}^{2+}$ (M)		Final solution		X-ray results
Starting solution	Final solution	Mg^{2+} (M)	Ca^{2+} (M)	
No Ca	8.94	0.177	0.0198	M (0 mole % Ca)
9.10	3.49	0.138	0.0395	M (0 mole % Ca) >> C
3.41	2.11	0.107	0.0508	M (12 mole % Ca)
				> P (49 mole % Mg)
1.52	1.06	0.0698	0.0661	D
0.57	0.55	0.0411	0.0742	C
0.25	0.26	0.0217	0.0843	C
0.11	0.13	0.0112	0.0898	C

intermediate high-magnesium calcite phase and aragonite through two intermediates, a low-magnesium calcite followed by a high-magnesium calcite in $\text{CaCl}_2 + \text{MgCl}_2$ solutions of $I=6$ at 252° to 295°C . In none of our experiments (all at seawater ionic strength) were any intermediate magnesium calcite phases observed.

The observation that dolomite forms rapidly from calcite in $\text{MgCl}_2 + \text{NaCl} + \text{CaCl}_2$ solutions (Tables 1 and 2) raises the question of why dolomite is not a more abundant phase in marine sedimentary rocks. The main reason for the scarcity of open marine dolomite, shown in our experiments, is that dissolved SO_4^{2-} is a very effective inhibitor of calcite dolomitization, even at concentrations less than 5 percent of its seawater value. The experimental solutions were below saturation with respect to anhydrite (the stable calcium sulfate mineral at 200°C). Although the inhibiting effect of SO_4^{2-} seems established, its mechanism is still unknown. We suggest that dolomite can form rapidly in nature only where SO_4^{2-} concentrations are low. The most effective process of SO_4^{2-} removal from marine pore waters is its microbial reduction in organic-rich sediments. This conclusion is strongly supported by the finding of extensive, early-diagenetic dolomites in organic-rich marine sediments (1), in which microbial SO_4^{2-} reduction was observed directly by chemical analyses of pore water (12) and indirectly by stable isotopic analyses of the solids (1, 3). The presence of SO_4^{2-} probably explains why dolomite is rare in some almost pure calcareous sediments where magnesium depletion by silica diagenesis is not an important process.

In sedimentary environments of rapid deposition (more than about 100 m per million years), diffusive communication of pore waters with seawater is precluded, and the extent of dolomite formation may be limited by the supplies of magnesium, calcium, or carbonate ions. Dolomite can form by the replacement of biogenic carbonate, a solution reprecipitation phenomenon (11), in which the supply of magnesium would be limiting. In organic-rich sediments, dolomite can form without solid carbonate being present. In this case, the most important sources of HCO_3^- would be from SO_4^{2-} reduction, methanogenesis, or fermentation; in these sediments, the calcium supply would very likely be limiting. The $\delta^{13}\text{C}$ values (relative to the Pee Dee belemnite standard) of these dolomites vary from negative to strongly positive (1, 3). Magnesium is abundant on ion-exchange sites in marine silicate-rich

Table 2. Results of kinetic experiments to determine the extent of dolomite (D) and protodolomite (P) formation from 20 mg of calcite (C) or aragonite (A) in 10 ml of $0.080M \text{MgCl}_2 + 0.060M \text{CaCl}_2 + 0.280M \text{NaCl}$ ($I = 0.70$) 200°C .

Starting solid	Duration (hours)	X-ray results
C	48	C >> P (46 mole % Mg)
C	112	P (46 mole % Mg) >> C
C	160	D
A	48	P (105), peak slightly broadened
A	112	D (105), peak sharp

Table 3. Effect of SO_4^{2-} on dolomite (D) or protodolomite (P) formation from 20 mg of calcite (C) in 10 ml of $0.080M \text{MgCl}_2 + 0.060M \text{CaCl}_2 + \text{NaCl} + \text{Na}_2\text{SO}_4$ ($I = 0.70$) 200°C , 2 weeks. The concentrations of Mg^{2+} and Ca^{2+} in the initial solution of $0.080M \text{MgCl}_2 + 0.060M \text{CaCl}_2$ correspond to a $\text{Mg}^{2+}/\text{Ca}^{2+}$ molar ratio of 1.33. Under this condition dolomite is the stable phase (Table 1).

Starting solution SO_4^{2-} (M)	X-ray results
0.0000	D
0.0010	P (43 mole % Mg) >> C
0.0020	C >> P (45 mole % Mg)
0.0030	C >> P (46 mole % Mg)
0.0040	C

sediments. The NH_4^+ , produced during SO_4^{2-} reduction, may exchange with magnesium, freeing the latter for dolomitization (13). A rough calculation, based on the assumption that (i) one Mg^{2+} is adsorbed per square nanometer of surface area (a maximum number), (ii) the surface area of opaline silica is $200 \text{ m}^2/\text{g}$, and (iii) the porosity is 75 percent, shows that about four times as much Mg^{2+} is available on exchange sites of solid silica as is dissolved in pore waters. Therefore, SO_4^{2-} reduction promotes dolomitization in three ways: (i) by removal of the dissolved SO_4^{2-} inhibitor, (ii) by production of alkalinity, and (iii) by production of NH_4^+ , which subsequently releases adsorbed Mg^{2+} .

Table 4. Effect of amorphous silica on dolomite and protodolomite formation. Starting solids were 100 mg of calcite (C) plus 100 mg of amorphous silica (Ludox) in 10 ml of $\text{MgCl}_2 + \text{NaCl}$ solution ($I = 0.70$) 200°C , 2 weeks; opal-CT, Op-CT.

Mg^{2+} (M)		Final solution Ca^{2+} (M)	Final solution		X-ray results
Starting solution	Final solution		$\text{Mg}^{2+}/\text{Ca}^{2+}$ (M)	H_4SiO_4 (mM)	
0.0000	0.0000	0.00158	No Mg		C
0.0209	0.0004	0.02121	0.02	12.504	C
0.0418	0.0043	0.03748	0.12	11.567	C >> Op-CT
0.0628	0.0054	0.05532	0.10	12.463	C >> Op-CT
0.0837	0.0061	0.07571	0.08	12.422	C >> Op-CT
0.1046	0.0109	0.08934	0.12	12.259	C >> Op-CT

As shown in Table 4, the transformation of opal-A to opal-CT may also retard CaCO_3 dolomitization through the formation of unidentified nuclei which contain Mg^{2+} and OH^- and enhance opal-CT formation (7, 14). The rather common association of chert with dolomite implies that the Mg^{2+} taken up by the opal-CT is eventually released during the transformation of opal-CT to quartz, promoting the formation of dolomite.

The "classical" models of dolomite formation are as follows: (i) evaporative reflux (15), (ii) evaporative pumping (16), (iii) mixed water or schizohaline (17), and (iv) shale dewatering with connate water expulsion by compaction (18). In all these environments, the $\text{Mg}^{2+}/\text{Ca}^{2+}$ ratio was thought to be the controlling factor: the higher the ratio, the more favorable for dolomitization. We propose that dolomitization is not primarily controlled by the $\text{Mg}^{2+}/\text{Ca}^{2+}$ ratio. Dolomite is already the stable carbonate phase in seawater (18) and in many interstitial waters. McKenzie *et al.* (19) pointed out that dolomite occurs in the intermediate sabkha of Abu Dhabi, where $\text{Mg}^{2+}/\text{Ca}^{2+} = 2.5$ to 7.0 , but not in the areas of frequent (almost daily) flood recharge from marine waters, even though there $\text{Mg}^{2+}/\text{Ca}^{2+} = 7.0$ to 27.0 [but the SO_4^{2-} concentration is also higher (20, 21)]. It is instead the decrease of dissolved SO_4^{2-} by calcium sulfate precipitation and concurrent bacterial SO_4^{2-} reduction, or through mixing of seawater or modified connate water with fresh water, that allows dolomite formation in these environments. As reported by Butler (20), the majority [72 percent of sample line 1 in (20)] of samples of sabkha brines associated with gypsum-anhydrite and dolomitized-aragonite sediments have SO_4^{2-} concentrations significantly below the seawater concentration of $0.028M$. Half contain only 0.003 to $0.015M$ dissolved SO_4^{2-} . The fact that the SO_4^{2-} content of 28 percent of the sabkha brines is higher than that of seawater does not invalidate our conclusion, as there is no proof that dolomitiza-

tion took place in contact with the modern brines. The relatively low SO_4^{2-} concentrations of most of these brines and the observation by Kinsman (22) that dolomitization does not occur in carbonate sabkhas composed mainly of calcite skeletal grains support our experimental results. Minor amounts of dissolved SO_4^{2-} strongly inhibit calcite dolomitization, whereas dolomitization of aragonite (the dominant CaCO_3 phase in most carbonate sabkhas) may still proceed at somewhat higher dissolved SO_4^{2-} concentrations. This explanation applies equally well to continental lacustrine environments, such as the Green River Formation, Wyoming, where large amounts of dolomitic mudstones are associated with both the oil shales and evaporites (23).

PAUL A. BAKER
MIRIAM KASTNER

Scripps Institution of Oceanography,
University of California, San Diego,
La Jolla 92093

References and Notes

1. K. A. Pisciotto and J. J. Mahoney, *Initial Rep. Deep Sea Drill. Proj.*, in press; I. Friedman and K. S. Murata, *Geochim. Cosmochim. Acta* **43**, 1357 (1979).
2. Lists of the occurrences of minerals in DSDP cores were made available by D. Hawkins of the DSDP Data Processing Group.
3. K. R. Kelts and J. A. McKenzie, *26th Int. Geol. Conf.* (1980) (Abstr.); see also *Initial Rep. Deep Sea Drill. Proj.*, in press.
4. J. M. Gieskes, in *Initial Rep. Deep Sea Drill. Proj.* **25**, 361 (1974).
5. Aragonite was prepared by the method of J. L. Wray and F. Daniels, *J. Am. Chem. Soc.* **79**, 2031 (1957).
6. "Protodolomites" and "dolomites" as used throughout this report were defined by A. M. Gaines [J. *Sediment. Petrol.* **47**, 543 (1977)] and J. R. Goldsmith and D. L. Graf [J. *Geol.* **66**, 678 (1958)].
7. M. Kastner, J. B. Keene, J. M. Gieskes, *Geochim. Cosmochim. Acta* **41**, 1041 (1977).
8. P. E. Rosenberg and H. D. Holland, *Science* **145**, 700 (1964).
9. H. E. Usdowski, *Die Genese von Dolomit in Sedimenten* (Springer, Berlin, 1967).
10. A. M. Gaines [in *Concepts and Models of Dolomitization*, D. H. Zenger et al., Eds. (Soc. Econ. Paleontol. Mineral. Spec. Publ. 28) (Society of Economic Paleontologists and Mineralogists, Tulsa, 1980), p. 81] demonstrated in solutions of $I=2$ at 100°C that dolomite is stable at $\text{Mg}^{2+}/\text{Ca}^{2+} = 3$ to 7; furthermore, the rate of formation of dolomite was dependent on the value of $\text{Mg}^{2+}/\text{Ca}^{2+}$ being a maximum at about 5; P. E. Rosenberg, D. M. Burt, H. D. Holland, *Geochim. Cosmochim. Acta* **31**, 391 (1967).
11. A. Katz and A. Matthews, *Geochim. Cosmochim. Acta* **41**, 297 (1977).
12. J. M. Gieskes, *Initial Rep. Deep Sea Drill. Proj.*, in press.
13. ———, *Soc. Econ. Paleontol. Mineral. Spec. Publ.*, in press.
14. P. A. Baker, M. Kastner, J. D. Byerlee, D. A. Lockner, *Mar. Geol.* **38**, 185 (1980).
15. B. H. Purser, Ed., *The Persian Gulf* (Springer, Berlin, 1973); J. E. Adams and M. L. Rhodes, *Bull. Am. Assoc. Pet. Geol.* **44**, 1912 (1960); W. Fisher and P. Rodda, *ibid.* **53**, 55 (1969).
16. K. J. Hsü and C. Siegenthaler, *Sedimentology* **12**, 11 (1969).
17. R. L. Folk and L. S. Land, *Bull. Am. Assoc. Pet. Geol.* **59**, 60 (1975); K. Badiozamani, J. *Sediment. Petrol.* **43**, 965 (1973); B. B. Hanshaw et al., *Econ. Geol.* **66**, 710 (1971).
18. D. L. Langmuir, *Geochim. Cosmochim. Acta* **35**, 1023 (1971).
19. J. A. McKenzie, K. J. Hsü, J. F. Schneider, in *Concepts and Models of Dolomitization*, D. H. Zenger et al., Eds. (Society of Economic Paleontologists and Mineralogists, Tulsa, 1980), p. 11.
20. G. P. Butler, *J. Sediment. Petrol.* **39**, 70 (1969).

21. P. Bush, in *The Persian Gulf*, B. H. Purser, Ed. (Springer, Berlin, 1973), p. 395.
22. D. J. J. Kinsman, *Bull. Am. Assoc. Pet. Geol.* **53**, 830 (1969).
23. H. P. Eugster and R. C. Surdam, *Geol. Soc. Am. Bull.* **85**, 1733 (1974); H. P. Eugster and L. A. Hardie, *ibid.* **86**, 319 (1975).
24. We thank R. Garrison, Y. Bentor, J. Gieskes, and D. Kent for helpful discussions and reviews of the manuscript and S. Morson-Baker for stylistic comments. We owe particular thanks to

J. Gieskes, who aided us in many aspects of this research and supplied unpublished pore water data from the Gulf of California. Research was supported by Office of Naval Research contract USN/N00014-79-C-0152. Research in Table 2 was supported by NSF grant OCE78-09652. Research support was also provided by the Chevron Oil Field Research Company, La Habra, Calif.

28 January 1981; revised 26 March 1981

Thyrotropin-Releasing Hormone Improves Cardiovascular Function in Experimental Endotoxic and Hemorrhagic Shock

Abstract. *Thyrotropin-releasing hormone significantly improved cardiovascular function when it was injected intravenously into conscious rats subjected to experimental endotoxic or hemorrhagic shock. Because thyrotropin-releasing hormone appears to be a "physiologic" opiate antagonist without effects on pain responsiveness, it may provide therapeutic benefits in the treatment of shock or acute hypotension.*

We have demonstrated that the opiate antagonist naloxone significantly improves cardiovascular performance and survival in experimental shock caused by endotoxemia (1–3), hemorrhage (4, 5), or spinal-cord injury (6, 7). This therapeutic action of naloxone in shock appears to be mediated by way of a blockade of endorphin action at opiate receptors within the central nervous system (6). However, receptor-level opiate antagonists such as naloxone may have the adverse effect of intensifying posttraumatic pain by inhibiting endorphin-mediated analgesia even as they improve the shock state. In contrast to naloxone, thyrotropin-releasing hormone (TRH) does not bind to opiate receptors, although it has selective activity in opposing many opiate-mediated effects (8). More specifically, TRH reverses behavioral and neuroendocrine changes produced by β -endorphin without altering the antinociceptive responses to either β -endorphin (8) or morphine (9). This ability of TRH to reverse the pharmacological and physiological effects of en-

dorphins without modifying analgesia prompted us to examine its possible therapeutic utility in experimental shock.

Tail-artery and external jugular vein cannulas were implanted in male Sprague-Dawley rats (250 to 300 g; Zivic-Miller Laboratories) as previously described (1). Twenty-four hours later, the arterial cannula was connected to a microtransducer (Narco Biosystems RP1500 attached to a Beckman physiograph, type R). This arrangement permitted continuous measurement of blood pressure and heart rate in awake, freely moving rats in their home cages.

In control rats, which were not subjected to shock, the cardiovascular effects of intravenous TRH alone were determined. After injecting the TRH (2 mg/kg; Beckman Labs.) we flushed the cannula with 0.2 ml of saline to ensure complete drug delivery. Cardiovascular variables were monitored for 45 minutes. The administration of TRH caused a significant increase in mean arterial pressure (MAP) of 11.1 ± 1.5 mm-Hg ($N = 10$, $t = 7.25$, $P < .001$; Student's t -test), with peak effects observed at 5 minutes after injection and persisting for 30 minutes (Fig. 1). Heart rate and pulse pressure were also significantly increased by this dose of TRH in all experiments (data not shown).

A second group of rats was subjected to endotoxic shock by the intravenous administration of *Escherichia coli* lipopolysaccharide endotoxin (15 mg/kg; Difco, control No. 654109) (1). In these animals, MAP fell precipitously at varying times over the next hour to 67 to 70 mm-Hg (1), which was approximately 26 percent (24 mm-Hg) below baseline levels of 92.7 ± 1.9 mm-Hg ($N = 22$). These rats, randomly divided into two groups, were then immediately injected

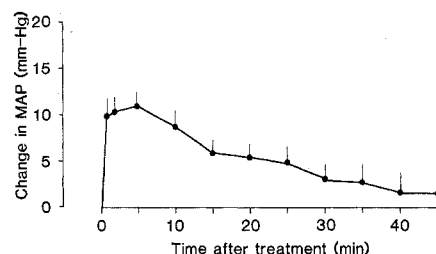


Fig. 1. The effects of intravenously administered TRH (2 mg/kg) on mean arterial pressure (MAP) in conscious, freely moving rats. Within seconds after the TRH injection there was a rapid increase in MAP. Vertical bars indicate the standard error of the mean, $N = 8$ rats; data are expressed as changes in MAP compared to values before treatment.